Land Cover Mapping at Sub-Pixel Scales: Unraveling the Mixed Pixel

Yasuyo Makido and Ashton Shortridge

Department of Geography, Michigan State University,
East Lansing, MI 48823 USA
Email: makidoya@msu.edu

Abstract

This study investigates the "pixel-swapping" optimization algorithm for predicting sub-pixel land cover distribution. Two limitations of this method, the arbitrary spatial range value and the arbitrary exponential model of spatial autocorrelation are assessed. Various weighting functions, as alternatives to the exponential model, are evaluated in order to derive the optimum weighting function. Two different simulation models were employed to develop spatially autocorrelated binary class maps. These rasters were then resampled to generate sets of representative medium resolution class maps, along with the initial "ground truth". Prior to conducting the sub-pixel allocation, the relationship between cell resolution and spatial autocorrelation, as measured by Moran's *I*, was evaluated. The form of this relationship was found to depend upon the simulation model. In all tested models, Gaussian, Exponential, and IDW, the pixel swapping method improved classification accuracy compared with the initial random allocation of sub pixels. However the results suggested that equal weight could be used to maximize accuracy and sub-pixel spatial autocorrelation instead of using these more complex models of spatial structure.

1. Introduction

One of the great challenges of modeling land cover using remotely sensed imagery is the mixed pixel problem: the problem that the level of spatial detail captured is less than the amount of detail that we would like, and that this sub-pixel level heterogeneity is important but not readily knowable. Traditionally, each pixel is classified into one of many land cover types (hard classification), implying that land cover exactly fits within the bounds of one or multiple pixels (Figure 1). However, many pixels consist of mixed land cover class composition. The solution to the mixed pixel problem typically centers on soft classification, which allows proportions of each pixel to be partitioned between classes. Sub-pixel class composition is estimated through the use of techniques, such as mixture modeling (e.g., Kerdiles & Grondona, 1996), supervised fuzzy c-means classification (e.g., Foody & Cox, 1994) and artificial neural networks (e.g., Kanellopoulos et al., 1992). The output of these techniques generally produces images that display the proportion of a certain class within each pixel. In most cases, this results in a more informative and less error prone representation of land cover than that produced using a hard, one-class-per-pixel classification (McKelvey & Noon, 2001).

However, the spatial distribution of these class components within the pixel remains unknown. The object of this paper is to overcome the mixed pixel problem by investigating a method for predicting sub-pixel land cover distribution.

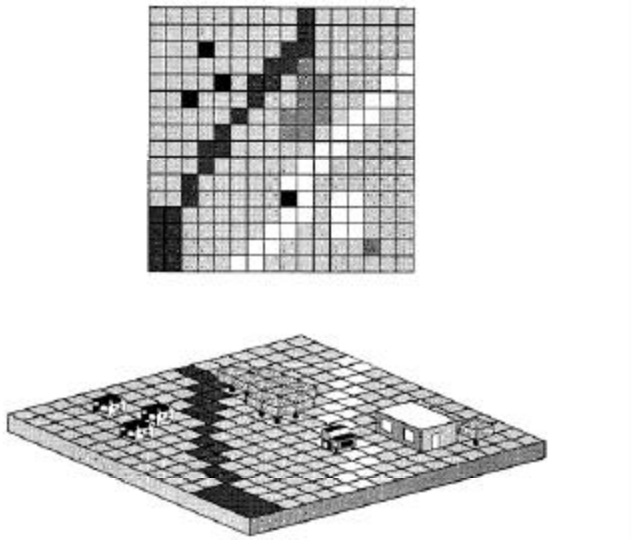

Figure 1. The pixel view of the world (From Fisher, 1997).

Several alternative algorithms have been proposed for allocating classes of sub-pixels. Aplin et.al (1999) developed a set of techniques to classify land cover on a per-field basis, rather than a traditional per-pixel basis, by utilizing the Ordnance Survey land line vector data. They concluded that the per-field classification technique was generally more accurate than the per-pixel classification. However, the necessity of accurate vector data sets limits this technique. Verhoeye and De Wulf (2002) introduced an approach that formulates the sub-pixel mapping concept as a linear optimization problem maximizing the spatial autocorrelation within the image. They produced a sharpened crisp land cover map without the need for finer spatial resolution data. The results showed a certain degree of success, but this non-iterative solution produced linear artifacts in the final map. Tatem et al. (2001, 2002) examined the application of a Hopfield neural network (HNN) technique to predict the spatial pattern of land cover features smaller/larger than the scale of a pixel by using information about pixel composition determined from soft classification. A Hopfield neural network was used as an optimization tool to make the output of a neuron similar to that of its neighboring neuron in order to maximize the spatial autocorrelation within the image. Tatem et al. (2003) applied the HNN technique to Landsat Thematic Mapper (TM) agricultural imagery to derive accurate estimates of land cover and reduce uncertainty inherent in such imagery. The study demonstrated that the spatial resolution of satellite sensor imagery does not necessarily represent a limit to the spatial detail obtainable within land cover maps derived from such imagery.

Atkinson (2001) examined the "pixel-swapping" optimization algorithm within a geostatistical framework as an alternative to the HNN algorithm. Like Verhoeye and De Wulf (2002) and Tatem et al (2001,2002,2003), Atkinson used the proportions of each land cover within each pixel to map the location of class components within the pixels.

Theses class proportions can be derived from various soft classification methods, which are described above. Unlike Verhoeye and DeWulf (2002), a "pixel-swapping" algorithm iteratively allocates sub-pixels to maximize the contiguity of the landscape.

Initially, this simple "pixel-swapping" algorithm randomly allocates class codes to sub-pixels. The spatial arrangement of sub-pixel values is iteratively changed based on a distance weighted function (attractiveness, O*i*) of each sub-pixel in order to maximize the correlation between neighboring sub-pixels. In this algorithm, the exponential weighting function is used to calculate the attractiveness:

$$Oi = \sum_{j=1}^{n} l_{ij} \cdot Z(X_j) \tag{1}$$

n: the number of neighbors

$Z(X_j)$: value of the binary class z at the jth pixel location Xj

l_{ij} : a weight predicted as:

$$l_{ij} = \exp(\frac{-h_{ij}}{a}) \tag{2}$$

h_{ij} : the distance between the pixel location for Xi and Xj

a : the range parameter of the exponential model

This simple algorithm is similar in character to simulated annealing. Simulated annealing is a family of optimization algorithms based on the principle of stochastic relaxation. An initial image is gradually changed so as to match constraints while honoring data values at their locations (Goovaerts, 1997). However, unlike the simulated annealing algorithm, which randomly selects two sites, the Atkinson's optimization algorithm deterministically selects the two sites most in need of swapping based on the attractiveness index *Oi*. Consequently, the pixel-swapping algorithm is relatively fast since convergence occurs in far less iterations. However, the choice of the exponential weighting function is arbitrary, and the value of the non-linear parameter of the exponential model (*a*) is experimentally derived. This paper reports on research to improve the pixel-swapping algorithm by considering alternatives to these two limitations.

Next, we describe how we test the parameters of this algorithm, and this is followed by the presentation of our results and discussion. The paper concludes with implication of our findings.

2. Methods

In this section, we introduce the data sets employed and discuss how we tested the various parameters of the Atkinson algorithm. The data sets described in the following were generated using C code developed by the authors, while Atkinson algorithm is implemented using custom code in the IDL programming language.

2.1. Simulation of Autocorrelated Images

This case study employs simulated binary images that have 315 rows and columns with substantial positive autocorrelation. Two methods are used. Both methods create binary raster files that are spatially autocorrelated at a level specified by a target Moran's *I* statistic set by the user (0.7, in both cases). Moran's *I* is an indicator of spatial autocorrelation for area data (Bailey & Gatrell, 1995). For a spatial proximity matrix (*W)* spatial correlation in attribute values (y_i) is estimated as:

$$I = \frac{n\sum_{i=1}^{n}\sum_{j=1}^{n} w_{ij}(y_i - \bar{y})(y_j - \bar{y})}{\left(\sum_{i=1}^{n}(y_i - \bar{y})^2\right)\left(\sum_{i\neq j}\sum w_{ij}\right)} \qquad (3)$$

The Moran index is positive when nearby areas tend to be similar in attribute, negative when they tend to be more dissimilar than one might expect, and approximately zero when attribute values are arranged randomly and independently in space (Goodchild, 1986).

Method One uses an initially random distribution, while Method Two uses a fractal model to rapidly initialize a highly autocorrelated surface. Then a cell-swapping algorithm is employed to shift the spatial arrangement to arrive at the specified *I*. Since these two methods result in notably different images despite the same Moran's *I* values, this study examines both simulated images (Figure 2, 3). We call the neutral image that is created by method one as Neutral A and that is created by method two as Neutral B. Both images contain 33 % of 1 (forest) and 67% of 0 (non-forest). In Neutral A, the forests patches are evenly distributed throughout the area. In Neutral B, the forest patches are larger and clumped at some locations. These images are aggregated to obtain coarser resolution images (Figure 4, 5). Therefore, we have "ground truth" available with which to test the results of these experiments on sub-pixel swapping.

Figure 2. Neutral A: Cell size 1

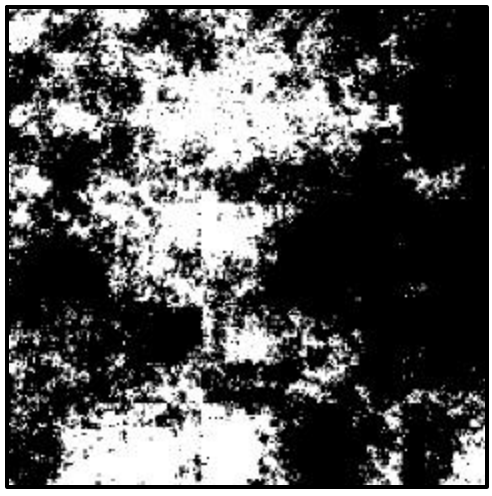

Figure 3. Neutral B: Cell size 1

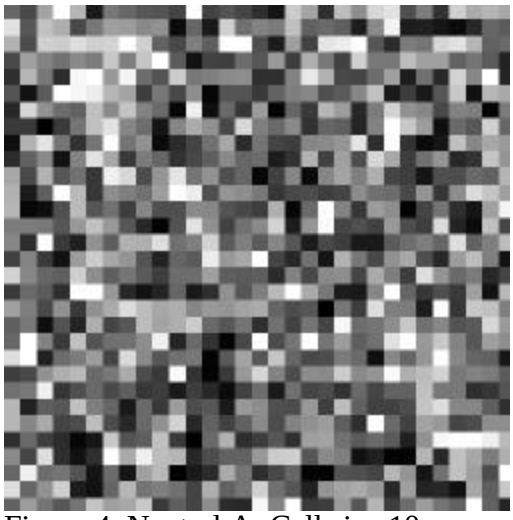

Figure 4. Neutral A: Cell size 10

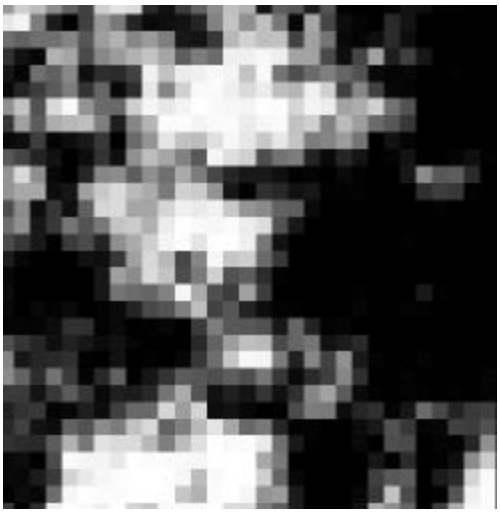

Figure 5. Neutral B: Cell size 10

2.2. Spatial resolution

In this study, we attempt to derive the optimum weighting function based on the degree of contiguity in the original map. Moran's *I* is used to characterize the structure of the landscape. However, geographic phenomena generally are scale-dependent, which means the analysis results could differ considerably if different pixel resolutions are used. This is known as the modifiable areal unit problem (MAUP). The fundamental sources of uncertainty in remotely sensed data are caused by interactions between the scale of variation within the ground scene and the spatial resolution of the sensor (Friedl et al. 2001). The relationship between the Instantaneous Field of View (IFOV) of the sensor system and the spatial variability in the landscape will strongly influence the types of analyses that may be performed. Thus, Moran's *I* is a function of spatial resolution and looking at a value calculated at the original pixel resolution may be misleading. Therefore, we quantify the effect of spatial resolution on the empirically calculated *I.*

The original Neutral A and B rasters, with cell sizes of 1, are resampled to cell sizes 2, 3, 4, ..., 10. These reduced-resolution version of images are generated by summation of the input cells that are encompassed by the extent of the output cell, as demonstrated in Figure 6. Note that the resulting cell value indicates the proportion of the cell occupied by class 1, matching the output of soft classification techniques.

0	0	0	0	0	0
0	1	1	1	0	0
0	1	1	1	0	0
0	1	1	1	0	0
0	0	1	1	0	0
0	0	0	0	0	0

→

4	2
3	2

Figure 6. Resampled cell size 3

The Moran's *I* for each resampled image is calculated for both Neutral A and B. The first goal of this paper is to examine how these Moran's *I* values change with the coarsening of the original fine images.

2.3. Spatial Weighting Functions

The Atkinson spatial weighting function can be expressed as a special case of the Exponential covariance model:

$$l_{ij} = \exp(\frac{-3h_{ij}}{r}) \tag{4}$$

h_{ij} : the distance between the pixel location for *Xi* and *Xj*
r : range of the covariance

The range is the lag distance at which pixels become independent of each other. Atkinson employs a = 5, which equates to a range of 15. In this study, various range values from 1 to 20 for the Exponential model are examined. As an alternative to the exponential model, the Gaussian model and the inverse distance weighting function (IDW) are examined. The weighting function using a Gaussian model is:

$$l_{ij} = \exp(\frac{-3h_{ij}^{2}}{r^{2}}) \tag{5}$$

The inverse distance weighting function is :

$$l_{ij} = \frac{1}{h_{ij}^{k}} \tag{6}$$

k : a real number

For the Gaussian model, various range values from 1 to 20 are examined. For IDW model, various k values from 0 to 10 are examined.

In addition to testing the various spatial weighting functions, an equal weight function is examined. Attractiveness *Oi* can be modeled simply as the sum of the values at the nearest neighbors.

$$Oi = \sum_{j=1}^{n} Z(X_j) \tag{7}$$

n: the number of neighbors
$Z(X_j)$: value of the binary class z at the *j*th pixel location *Xj*

This simplified attractiveness makes the algorithm simpler and probably faster.

In this study, the resampled coarse resolution images, which have cell sizes of 5 and 7, are used to reproduce cell size 1 fine resolution image. For those with cell size 7, the number of iterations used is 13 and for those with cell size 5, the number of iterations used is 9. The number of nearest neighbors used is 24 (the second neighbor) for both cell sizes.

In all cases, Moran's *I* is used as an index of the spatial contiguity of the landscape, and Percent Correctly Classified (PCC) is used as a classification accuracy assessment. PCC is calculated by the ratio of the sum of correctly classified sub-pixels in all classes to the sum of the total number of sub-pixels.

3. Results and Discussion

Figure 7 shows the relationship between Moran's *I* and resampled coarse resolution images for both neutral images. In the case of Neutral A, as the resolution decreases, Moran's *I* decreases, which means the image is less autocorrelated than the original one. In the case of Neutral B, Moran's *I* does not change much with the resolution change, and all *I* values are higher than that for the original image, which means the coarsened image is more autocorrelated than the original one. While the two original neutral images have the same Moran's *I* value, the pattern of spatial distribution are quite different: for Neutral A, the patches are distributed evenly throughout the area, and for Neutral B, the patches are large and clumped at some areas. Therefore, as the images are coarsened, the distribution differences become more apparent. Thus, the Moran's *I* value is dependent on the underlying process generating the autocorrelated pattern and, therefore, characterizing the relationship between resolution and Moran's *I* will be challenging without knowing the distribution pattern of the landscape.

Figure 8 demonstrates the effectiveness of the pixel-swapping method through iteration using the exponential model. Classification accuracy and Moran's *I* increase until iteration 13 and level off for both neutral images for cell size 7. The results imply that the algorithm successfully attempts to increase the degree of spatial autocorrelation, and improves classification accuracy within a pixel. Cell size 5 images show similar results. However, the appropriate iteration number increases with the resampled cell size increase, since there are more sub-pixels to be swapped within a pixel. For the following examination, iteration 13 for cell size 7 and iteration 9 for cell size 5 are used.

For the Exponential and the Gaussian model, range values from 1 to 20 are tested. Moran's *I* and classification accuracy increase initially and then level off (Figure 9, 10). Although the graph for the IDW model has a quite different appearance to the other models (Figure 11), it implies the same meaning as the other models. All results suggest that as the weight becomes more similar, Moran's *I* and overall accuracy increase. Therefore, we also tested the equal weight function (Figure 12).

The figures demonstrate that the equal weight function can produce similar results to the original exponential model. Thus, employing an equal weighting scheme appears preferable since it can produce similar results and may also be computationally faster than using a weighting function.

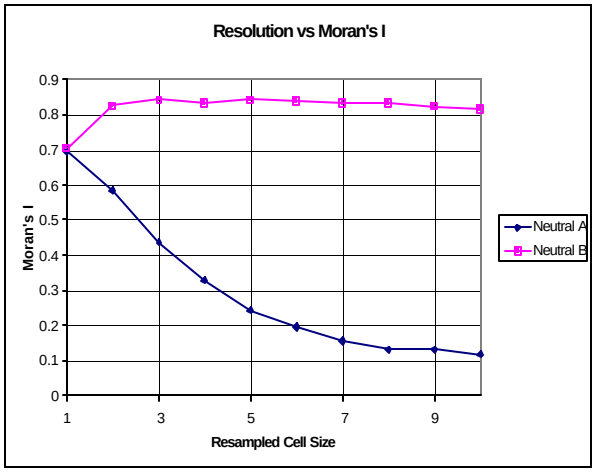

Figure 7. Resolution test

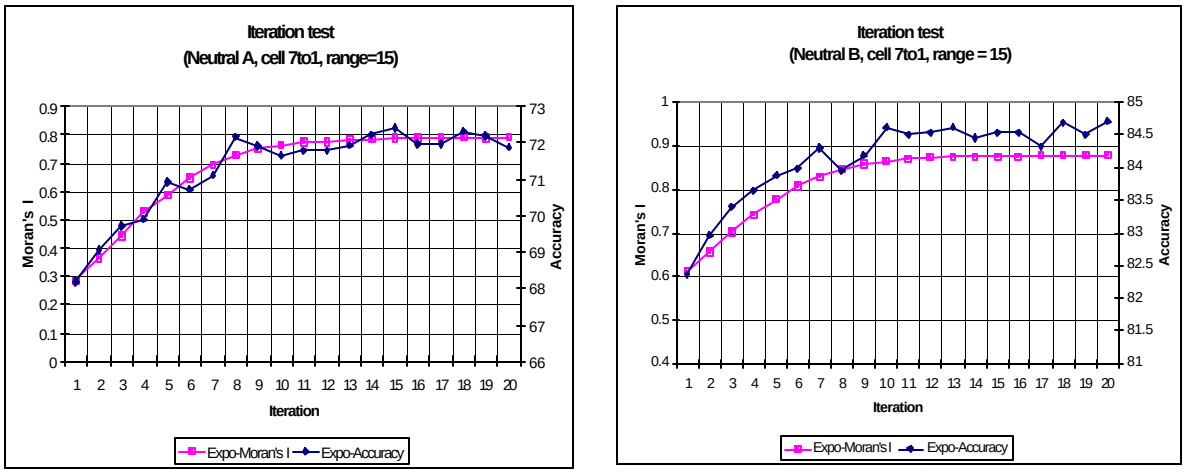

Figure 8. Iteration test (Exponential, cell 7to1, range=15)

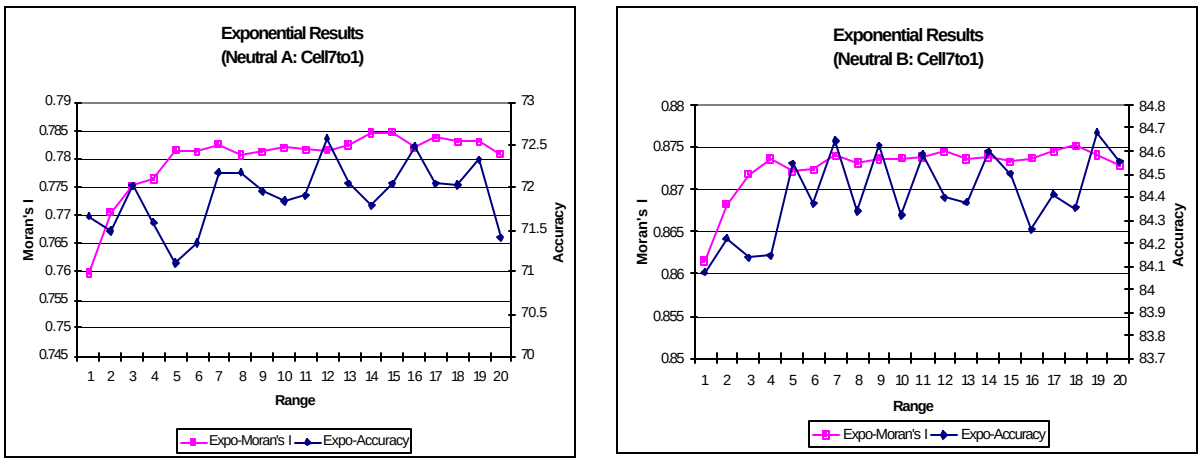

Figure 9. Range test (Exponential, cell 7to1)

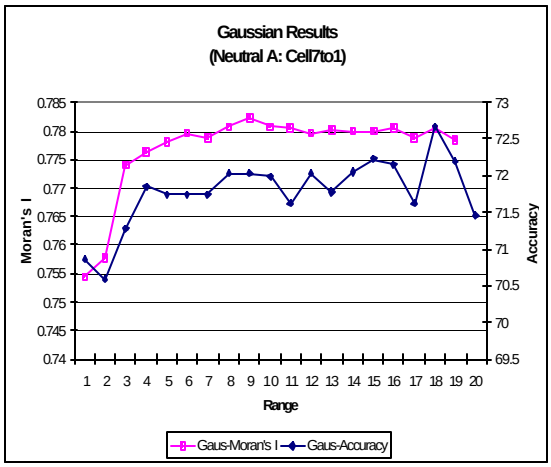

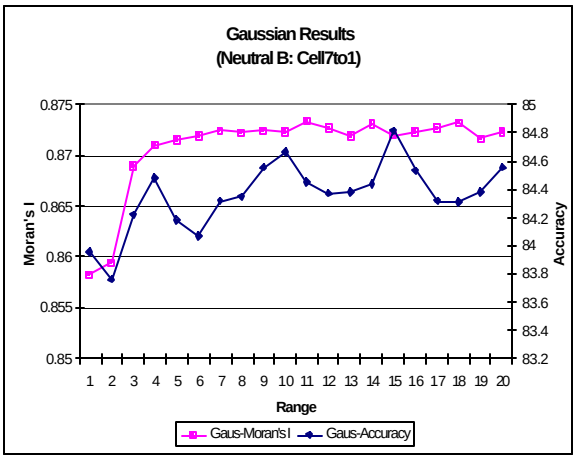

Figure 10. Range test (Gaussian, cell 7to1)

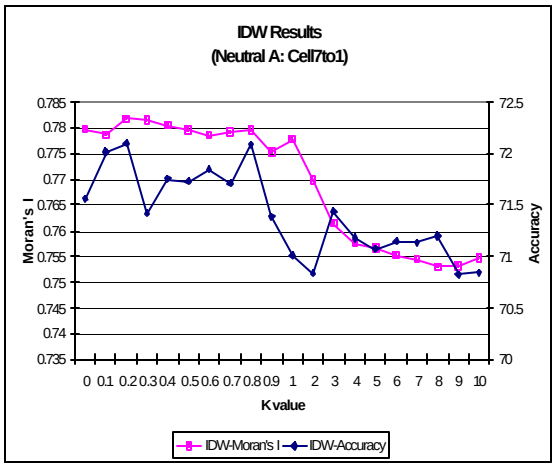

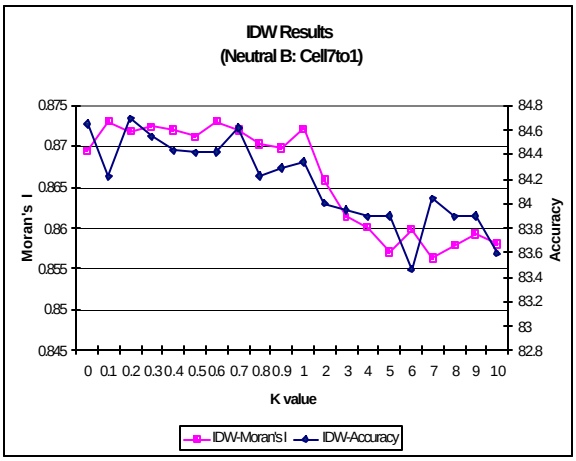

Figure 11. K-value test (IDW, cell 7to1)

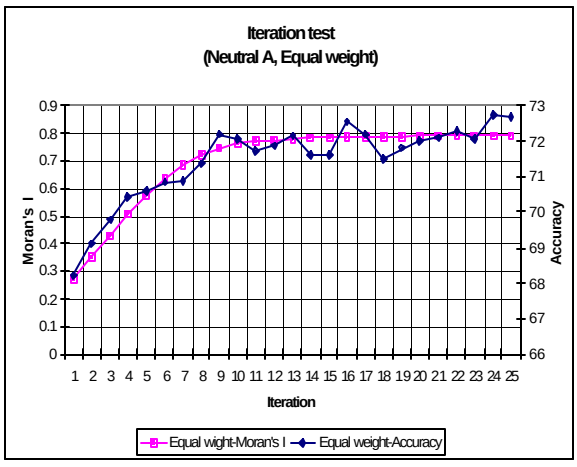

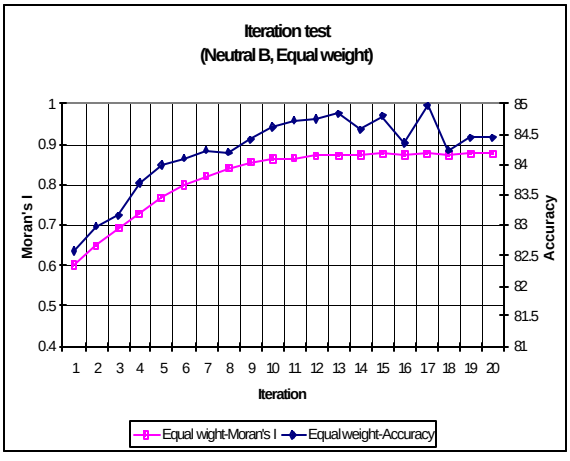

Figure 12. Iteration test (Equal weight, cell 7to1)

4. Conclusions

This study investigates the "pixel-swapping" optimization algorithm for modeling sub-pixel land cover distribution. We examine the effect of spatial resolution on Moran's I and find that the relationship is highly image dependent: different underlying process models may give rise to images with identical Moran's *I* values but with very different spatial scaling properties. Two limitations of this method, the arbitrary spatial range value and the arbitrary exponential model of spatial autocorrelation, are assessed. Various weighting functions, as alternatives to the exponential model, are evaluated in order to derive an optimum weighting function. In all tested models, Gaussian, Exponential, and IDW, the pixel swapping method improves classification accuracy compared with the initial random allocation of sub pixels. However the results suggest that equal weights could be used to maximize accuracy and Moran's *I* value instead of using more complex models of spatial structure.

One limitation of the pixel-swapping method relates to the fact that the algorithm works best for highly contiguous landscapes like these in this study, since the algorithm attempts to maximize the spatial autocorrelation. However, not all landscapes are highly contiguous. Therefore, it is necessary to investigate methods to incorporate the degree of autocorrelation of the landscape (if such information is available) without maximizing the autocorrelation.

Several potential avenues for further research present themselves. In this study, Moran's *I* is used as an index of the spatial contiguity of the landscape, and Percent Correctly Classified (PCC) is used as a classification accuracy assessment. There are alternative ways to characterize landscape. Various landscape indices, such as mean patch size, number of patches, and total edge length, can be used. These indices are employed to quantify landscape structure in terms of landscape configuration and landscape composition (Haines-Young & Chopping, 1996). The effect of sub-pixel models on these alternative metrics is unknown; they may show markedly different behavior than the results for Moran's *I* identified in this work. Alternatively, the employment of different metrics may provide a much richer basis for modeling landscape pattern at the sub-pixel scale.

A second issue involves the complexity of the problem under examination. This research only considered binary class maps (e.g. forest/non-forest). Since our models of the landscape, in general, are composed of a variety of land cover types, it is vital to investigate ways to handle multiple cover classes at the sub-pixel level.

The "pixel-swapping" approach can benefit researchers who employ remote sensing imagery. In many cases, the satellite sensor that provides large spatial coverage has insufficient spatial detail to identify landscape patterns. Therefore, application of the super-resolution technique described in this paper could potentially solve this problem by providing detailed land cover predictions from relatively coarse resolution satellite sensor imagery.

6. References

Aplin, P., Atkinson, P.M., and Curran, P.J. 1999. Fine spatial resolution simulated satellite imagery for land cover mapping in the United Kingdom. *Remote Sensing of Environment*. 68 pp.206-216.

Atkinson, P.M. 2001. Super-resolution target mapping from soft-classified remotely sensed imagery. *Geocomputation*. http://www.geocomputation.org/2001/papers/atkinson.pdf.

Bailey, T.C., and Gatrell, A.C. 1995. *Interactive spatial data analysis*. Longman Scientific & Technical, Harlow Essex, England.

Fisher, P. 1997. The pixel: a snare and a delusion. *International Journal of Remote Sensing*. 18 (3) 679-685

Foody, G.M., and Cox, D.P. 1994. Sub-pixel land cover composition estimation using a linear mixture model and fuzzy membership functions. *International Journal of Remote Sensing*. 15 (3) 619-631.

Friedl, M.A., McGwire, K.C., and McIver, D.K. 2001. An Overview of Uncertainty in Optical Remotely Sensed Data for Ecological Applications. *Spatial uncertainty in ecology : implications for remote sensing and GIS applications*, edited by C.T. Hunsaker, M.F. Goodchild, M.A. Friedl, T.J.Case. New York : Springer pp.258-283.

Goodchild, M.A. 1986. *Spatial Autocorrelation*. CATMOG 47. Geo Books, Norwich, UK

Goovaerts, P. 1997. *Geostatistics for Natural Resources Evaluation*. Oxford University Press, New York.

Haines-Young, R., and Chopping, M. 1996. Quantifying landscape structure: a review of landscape indicies and their application to forested landscapes. Progress in Physical Geography 20(4): 418-445.

Kanellopoulos, I., A. Varfis, G. G. Wilkinson, and J. Megier. 1992. Land cover discrimination in SPOT imagery by artificial neural network-a twenty class experiment. *International Journal of Remote Sensing* 13(5): 917-924.

Kerdiles, H., and Grondona, M. O., 1995. NOAA- AVHRR NDVI decomposition and subpixel classification using linear mixing in the Argentinean Pampa. *International Journal of Remote Sensing*, 16(7), pp. 1303-1325.

McKelvey, K.S., and Noon, B.R. 2001. Incorporating Uncertainties in Animal Location and Map Classification into Habitat Relationships Modeling. *Spatial uncertainty in ecology : implications for remote sensing and GIS applications*, edited by

C.T. Hunsaker, M.F. Goodchild, M.A. Friedl, T.J.Case. New York : Springer pp.72-90.

Tatem,A.J., Lewis, H.G., Atkinson, P.M., and Nixon, M.S. 2001. Super-resolution target identification from remotely sensed images using a Hopfield neural network. *IEEE Transactions on Geoscience and Remote Sensing*. 39 pp.781-796.

Tatem,A.J., Lewis, H.G., Atkinson, P.M., and Nixon, M.S. 2002. Super-resolution land cover pattern prediction using a Hopfield neural network. *Remote Sensing of Environment*. 79 pp.1-14.

Tatem,A.J., Lewis, H.G., Atkinson, P.M., and Nixon, M.S. 2003. Increasing the spatial resolution of agricultural land cover maps using a Hopfield neural network. *International Journal of Geographical Information Science*. 17 (7) pp.647-672.

Verhoeye, J., and De Wulf, R. 2002. Land cover mapping at sub-pixel scales using linear optimization techniques. *Remote Sensing of Environment*. 79 pp.96-104.